

# Exergetic Performance Assessment of a Double-Flash Geothermal Power Plant in Puga Valley, India

Haloi. Prabin, Kumar. Ankit, Dutta. Joyshree and Makunike. Desire Fadzi

*Department of Mechanical Engineering, Tezpur University, India.*

Received Date 20 September 2023; Revised Date 18 November 2023; Accepted Date 23 November 2023

\*Corresponding author: haloi\_p@tezu.ernet.in (H. Prabin)

## Abstract

The application of a geo-fluid is primarily characterized by its geo-field conditions and locations. One such application of geo-fluid is in power generation using suitable energy conversion systems. In this study, a thermodynamic model of a double-flash geo-thermal power plant (DFGPP) has been developed to evaluate its performance, which is mainly based on the geo-fluid of the Puga valley of Ladakh region in the Indian peninsula. The present study investigates the possible use of the DFGPP in the region through application of the exergy tool of the second law of thermodynamics. Under the Puga geo-fluid conditions, the energy and exergy rates, thermal losses, exergy destruction, and thermal and exergetic efficiencies are evaluated. From the thermal analysis results of the DFGPP, the condenser has the maximum energy loss with 97.08% of the overall loss, followed by low pressure turbine (LPT) and the high pressure turbine (HPT) with minimal energy rate losses of 2.28 % and 0.63 %, respectively. However, negligible losses in energy are found to occur in the mixing devices, pump, and the fluid separators. The maximum rate of exergy destruction occurs in the LPT with 38.95 % and least in the low pressure separator (LPS); the DFGPP operated with energy and exergy efficiencies of 9.52% and 48.39% approximately, producing a net output work of 3.9 MW. The overall cycle exergy destruction is found at 5.4% of the total energy losses. The use of DFGPP systems in the Puga geo-field can be a suitable option in power generation.

**Keywords:** *Double flash, Energy rate, Exergy destruction, Exergetic performance assessment, Exergetic efficiency.*

## 1. Introduction

The rise in world population and the need of continuous economic development has created huge impact on our scarcely available fossil fuel energy resources seeking increased energy supply. The ongoing depletion of fossil fuel reserves has now made it a limited energy resource, and the repeated extraction from these reserves created huge worldwide problems with energy security and sustainability. These actions have extremely harmful environmental effects including climate change and global warming. As such, the world currently face difficulties related to climate change and energy security, and it has become crucial to investigate the possibilities of transition to alternative energy sources in order to establish a sustainable future for the globe. One option to reduce the current energy crisis considerably is by using renewable energy sources such as solar, wind, hydropower, ocean and tidal energy, and geo-thermal energy. These energy sources are abundant, environmental friendly, and produce

little to no greenhouse gases (GHGs). Among these resources, geo-thermal energy is a promising renewable energy that is dependable and sustainable. This source of power has the ability to supply a large portion of the world's energy needs. It is estimated that by 2050, geo-thermal energy will be able to meet up to 3.5% of the world's energy demands [1]. Geo-thermal energy is produced from the inherent heat of the Earth's core. The sources of this energy include the heat generated during the early phases of the earth's genesis and the radioactive decay of its elements. The occurrences of these energy reserves require certain favourable geological conditions, and are mostly found around places of geo-tectonic plate interactions. Though, different countries have started initiatives to explore and harness this energy; however, the full scale exploration of these geo-thermal energy reserves has not been possible so far. There are a number of geo-thermal energy sites found in India, which

can serve to produce enormous energy in the near future. These Indian geo-thermal sites have got great potential for harnessing the inherent geo-energy. The exploration of these geo-fields has led to the initiation of setting up of geo-thermal power stations.

The geo-thermal power plants can be operated as dry steam, flash steam, binary cycle type, etc. for electricity generation, heating, and cooling. Geo-thermal power production technologies used globally including enhanced geothermal systems (EGS) has been highlighted [2] and the cost and financing of geothermal energy power plants discussed by highlighting the advantages and disadvantages of each technology. The dry steam type is the oldest and most basic form of geothermal power plant using steam extracted directly from subsurface reservoirs that powers turbine and generates energy. These are suitable in areas with high-temperature geo-thermal resources. The flash steam type is the commonly used form of geo-thermal power plant in areas with low temperature geo-thermal resources. It uses steam to power the turbines from a separator, where the geo-fluid is flashed into steam and hot liquid fluid. The binary cycle type is the newest and most efficient form of geo-thermal power plant. It uses a heat exchanger to transfer heat from the geo-thermal fluid to a secondary fluid having a lower boiling point. This fluid is subsequently evaporated, and the energy produced from its vapours is used to run a turbine. Binary cycle power plants are more eco-friendly and less prone to corrosion as the geo-fluid is not directly used to generate electricity.

Geo-thermal power plants have been installed across various countries and studies conducted to evaluate the functioning, efficacy, and potential of these plants as an energy source. A number of geo-thermal fields located across the world have been studied to understand their geo-chemistry and geothermics. The potential and hindrances of such systems were discussed [3], while reviewing the geothermal energy resources and systems. A detail study of the EGS system in the Geysers geothermal field [4] reported that setting up of EGS systems would enhance the amount of energy production. There are several studies that analyzed geothermal power systems to determine the inefficient components, amount of energy losses, and their causes and discussed ways for enhancing efficiencies. These studies evaluated the thermodynamic performances of geo-thermal systems and their sustaining capability through the application of exergy analysis tool. Exergy analysis is a highly useful technique when the

thermodynamic studies through energy analysis alone are insufficient. It improves analytical accuracy and enables the identification of crucial process parameters. In a comparative study of the energy efficiency of several geothermal power systems [5], the performance indices and applicable conditions of single flash, double flash, binary cycle, and flash-binary systems were discussed. The study reported that a flash-binary power system operates at its best when the geo-fluid temperature lies between 100 °C and 150 °C. The study also emphasised the importance of energy analysis in assessing the sustainability and ecological effects of these power facilities. Using energy and exergy analysis, the exergy loss rates in several components of a double flash cycle were evaluated [6], and the optimal operating pressure for the LPS was obtained. The results of this analysis showed that introduction of a double-flash system will improve the efficiency and power generation capacity of the plant. In a similar study [7], the exergetic performance of a double-flash geo-thermal power plant in Sabalan was investigated. They computed the reservoir enthalpy and mass flow rate of the geo-thermal fluid, optimised the net power output, and identified the locations and amounts of exergy losses and destructions in the various operations within the facility. The study revealed that the condenser, low pressure turbine, low pressure separator, and waste brine are the areas where energy is destroyed most quickly. Using exergetic performance analyses of varying flashing from single to quadruple for geo-thermal power plants, the ideal flashing pressures and the total power outputs, as well as the energy and exergy efficiency were evaluated by Siddique and Dincer [8]. The study observes that as the number of flashing stages is raised from one to two, the power output grows more quickly. On the other hand, a considerable decrease in power output was seen when the flashing stages are raised from 2 to 3 and 3 to 4. Moreover, it has been reported that as the number of flash stages increases, both the energetic and exergetic efficiency decreases. From the results of the study, it was concluded that a double-flash steam power plants will be more advantageous than a triple or a quadruple flash type.

One of India's most intriguing geo-thermal sites is Puga, which is situated in the Changthang region of Jammu and Kashmir in northern India that has been examined in numerous studies [9-15]. Due to the location's extremely large temperature gradient, it has sufficient potential for geo-thermal energy extraction to produce power in a geo-

thermal plant. With field limitations and the geological structural context taken into account, Puppala and Jha [10] offered alternative extraction techniques for the utilisation of the Puga geo-thermal reservoir in their study. The evaluation of a possible geothermal reservoir depends on the conceptual model that controls fluid flow and heat transmission in the reservoir and such models of the Puga geothermal field has been suggested [11, 12]. Reservoir modeling of the Puga geo-thermal site has also been discussed [13]. In another work, Abdul and Harinarayana [14] mapped the properties of the Puga geo-thermal field using magnetotelluric (MT) experiment. These studies offer insightful information about the thermal potential of the Puga Valley geo-thermal field, and can be used as a starting point for additional study and advancement of geo-thermal energy production in India. Moreover, the geo-chemistry and mineralogy of the Puga geothermal field were examined [15], and found significant energy production potential in the reservoir fluids. Further, the geo-physical conditions of the Manikaran geothermal field in the Kullu valley, India, was studied [16]. Similarly, examination in the Tatapani geo-thermal field, Mandi, was initiated to determine the field's subsurface temperature [17]. Investigations at the Bakreshwar and Tantloi geo-thermal field have been reported [18] that examined the geo-chemistry of the thermal springs in these fields. It was estimated that these geo-thermal sites have the potential to generate at least 500 MWe of electricity.

However, such estimates are dependent on the rate of fluid flows, geo-thermal gradient, and the flow of heat. Moreover, the developments of geo-thermal power plants in India are in an early stage, and have been subjected to various constraints. Government assistance, thorough investigation and assessment of geothermal resources are some of the primary requirements for their successful installation. With a focus on Manikaran field in the Kullu region, a thermodynamic feasibility study of a combined cycle was conducted [19] for cold storage and power generation. The study found that utilizing low temperature geo-thermal heat sources served to be beneficial for variable refrigeration and power output. Utilising thermodynamic principles, an investigation on the technical viability of a geo-thermal power plant at Tatapani geothermal field [20] found that the area has enormous potential for the production of renewable energy. Thus it is observed that the energy and exergy assessments of geo-thermal plants are useful for understanding the potential of the geothermal reserves as well as for detection

and quantification of the inefficiencies that may result in the wastage of these energy reserves. The application of these analyses to geo-thermal power plants is anticipated to become increasingly crucial in maintaining their long-term sustainability and competitiveness, as is clear from the numerous studies, as the demand for renewable energy continues to rise.

Studies on the performance evaluation of double flash geo-thermal power plants could be found in available literature pertaining to different geo-fields located in other regions and conditions of the world. Moreover, India's geo-thermal sites have recently been focused on thermodynamic studies that are primarily aimed at increasing effectiveness and lowering environmental impacts. However, in the Indian context, studies of the geothermal fields are mostly concentrated in understanding the geo-fluid conditions and the energy potential of these fields. As to the authors' best knowledge, a thermodynamic performance evaluation of a DFGPP using the exergy analysis has not been fully and clearly addressed in the available literature under Indian context. Thus in the present study, a DFGPP is investigated exergetically to examine its thermodynamic performance using the available geo-fluid conditions and properties found in the Puga geo-thermal field reservoirs, which by itself is rare and incomplete in the available literature.

## **2. System description**

The DFGPP is analyzed to evaluate its performance under the available geo-fluid operating conditions in the Puga valley of Ladakh geofield area in the Indian sub-continent. The exergetic performance parameters are computed, which is defined by the second law of thermodynamics. The application of mass, and energy and exergy balance to the flow streams in and out of the components of the DFGPP provided a measure of the quality of the geothermal energy. The proposed DFGPP configuration is shown in Figure 1. The DFGPP system consists of two expansion valves (EV1, EV2), two separators, one high pressure (HPS or SEP1) and another low pressure (LPS or SEP2) separator for separating the liquid and vapour streams twice, a high pressure turbine (HPT), a low pressure turbine (LPT), a condenser, a pump and two mixing devices (M1 and M2), respectively. The high pressure and temperature geo-fluid from the production well (PW) flows through the first expansion valve (EV1), resulting in a two-phase fluid flow at state 2 with production of steam due to the reduction in

pressure. The two-phase flow is then separated in the adiabatic separator (HPS), as hot liquid and vapour. The vapour is directed to flow across the HPT, while the high temperature hot geo-fluid is subjected to a second flash, and flows to LPS after passing through the valve EV2. In the HPT, steam expands to produce work ( $W_1$ ). The low pressure steams from the two separator then flows to the mixer M1 and enters the LPT at state 8. The low pressure steam generates additional work  $W_2$ . The fluid stream at state 9 is converted into liquid form in the condenser which is raised to mixer 2 pressure using a pump. The liquid flow at state 10 (LPS exit) and the flow at pump exit at state 12 are combined in the mixer M2, and is finally channelled to the injection well (IW).

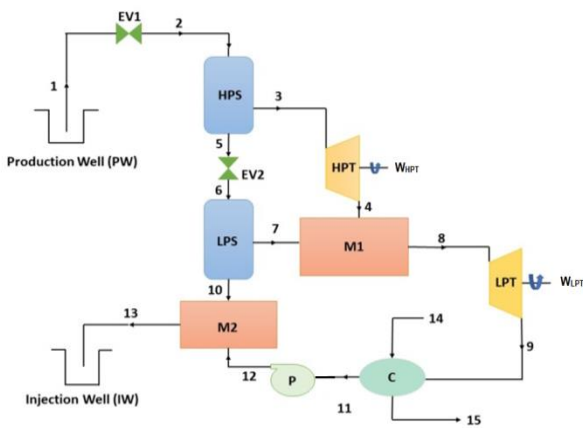


Figure 1. Schematic representation of the double flash geo-thermal power plant.

The variations in specific entropy of the flow streams in the DFGPP with respect to pressure and temperature are illustrated in Figure 2 by the T-s diagram.

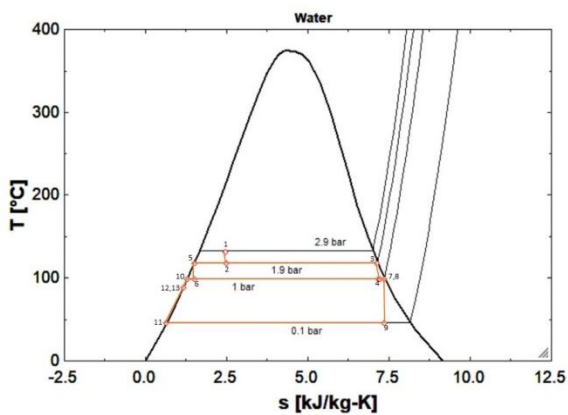


Figure 2. T-s diagram of flow streams for the DFGPP.

### 2.1. Mathematical formulation

The DFGPP is mathematically modeled using the mass and energy conservation concept and by applying the exergy balance to each component separately. The mathematical model of the

DFGPP has been framed considering similar models of other thermal systems, as discussed and illustrated in [21].

For the present DFGPP, certain assumptions are made [6, 7] for the convenience of analyses, which are given in the following:

- (i) Isentropic efficiency of turbines = 0.85
- (ii) Isentropic efficiency of pump = 0.60
- (iii) Condenser effectiveness = 100%
- (iv) Inlet temperature of cooling water to condenser = 25 °C
- (v) Outlet temperature of cooling water from condenser = 35 °C
- (vi) Pressure drop in expansion valve 1, EV1 = 1.0 bar
- (vii) Pressure drop in expansion valve 2, EV2 = 0.9 bar
- (viii) Condenser pressure = 0.1 bar
- (ix) No loss due to heat transfer
- (x) Mixing process is purely adiabatic in mixer 1 and 2
- (xi) Pressure drop across the separator is zero
- (xii) Pressure loss in the mixers 1 and 2 is negligible
- (xiii) The fluid is pumped to an injection pressure of 1 bar

### 2.2. Energy analysis

The mass and energy flows through the components of the DFGPP are evaluated by writing the mass and energy balance equations for each component. For the DFGPP system, it is assumed that flow through the control volume (CV) is of steady state steady flow (SSSF) type.

#### Mass balance

The mass conservation equations applied to the system components are evaluated using the Eqns (16-23) as given in Appendix A.

#### Energy balance

The energy rate balance equations for the system components' can be expressed in the context of the specific enthalpy,  $h$ , as follows:

#### Expansion valve 1 (EV1):

$$h_1 = h_2 \quad (1)$$

The specific enthalpy  $h_1$ , and the steam quality (dryness fraction) at state 2 can be expressed by equations (24-25); (see Appendix A, EV1), which are needed to calculate the mass flow rates of saturated vapor and saturated steam leaving the separator.

### High pressure separator (HPS/SEP1)

$$\dot{m}_2 h_2 = \dot{m}_3 h_3 + \dot{m}_5 h_5 \quad (2)$$

For the HPS/SEP1, the values of  $h_3$  and  $h_5$  can be evaluated using relations (26-27); (see Appendix A, HPS/SEP1).

### High pressure turbine (HPT)

For the HPT, the power output can be expressed by equation (3).

$$\dot{W}_{HPT} = \dot{m}_3 (h_3 - h_4) \quad (3)$$

The specific enthalpy and entropy of state 4 can be obtained using Eqns. (28-30); (see Appendix A, HPT) and equation (4):

$$h_4 = h_3 - \eta_T (h_3 - h_{4s}) \quad (4)$$

Here,  $\eta_T$  is the isentropic efficiency of the steam turbine, and the subscript  $s$  denotes the isentropic state.

### Expansion valve 2 (EV2)

The specific enthalpies at the states 5 and 6 and the steam quality for the EV2 has been obtained using the relations (31-32); (see Appendix A, EV2).

In a similar way, the energy balances for the Low Pressure Separator (LPS/SEP2), Mixing chamber (M1), Low pressure turbine (LPT), and the Condenser are evaluated using the relations (33-43) (see Appendix A).

### Pump

The pump work and pump isentropic efficiency can be obtained using the Eqns. (5-6) and using those given for pump (44-45); (see Appendix A).

$$\dot{W}_P = \dot{m}_{11} (h_{12} - h_{11}) \quad (5)$$

$$\eta_P = \frac{h_{12s} - h_{11}}{h_{12} - h_{11}} \quad (6)$$

where  $\eta_P$  is the isentropic efficiency of the pump, and  $v_{11}$  is the specific volume at state 11.

### Mixing chamber (M2)

The mixing processes for the mixer 1 and 2 are assumed adiabatic. Hence, for mixer 2, the specific enthalpy at state 13 will be obtained as given by equation (7) as:

$$h_{13} = \frac{\dot{m}_{10} h_{10} + \dot{m}_{12} h_{12}}{\dot{m}_{10} + \dot{m}_{12}} \quad (7)$$

### 2.3. Exergy analysis

The exergy model for the DFGPP is mathematically formulated using the exergy

balance for each component referring similar models [21-22] and with consideration of the component's energy model above.

For a steady-state steady flow (SSSF) process exergy balances are obtained by the following expressions:

For the state 'i', the specific flow exergy can be obtained by:

$$e_{x,i} = (h_i - h_o) - T_o (s_i - s_o) \quad (8)$$

and the corresponding exergy rate will be:

$$\dot{e}_i = \dot{m}_i [(h_i - h_o) - T_o (s_i - s_o)] \quad (9)$$

where  $T_o$  is the dead state temperature (= 298.15 K).

The exergy rate of individual components at a given state 'i' of the DFGPP can be balanced by its flow exergy rate and the exergy destruction rate as given by Eqns. (46-55); (see Appendix A, Exergy balance equations).

Thus the net power of the plant can be obtained by

$$\dot{W}_{net} = \dot{W}_{HPT} + \dot{W}_{LPT} - \dot{W}_P \quad (10)$$

Finally, the expressions (11) and (12) can be used to obtain the energy and exergy efficiencies:

$$\eta_{en} = \frac{\dot{W}_{net}}{\dot{m}_1 (h_1 - h_o)} \quad (11)$$

$$\eta_{ex} = \frac{\dot{W}_{net}}{\dot{e}_1} \quad (12)$$

### 3. Model validation

The results of the present DFGPP model is validated by considering two reference models- one of a flash-binary geo-thermal power generation system [23], and another one of a double flash geo-thermal power plant [7]. The results at the states 1 to 4 for the first flashing in the present study has been validated with data of [23], and is listed in table 1, while those for the second flashing considering the states 4 to 10 has been validated with the second reference model and are shown in table 2, respectively. Moreover, the validation with the second reference model is performed by taking input parameters of states 4 and 5 of [7]. From table 1, it is observed that under similar temperature, pressure and the mass flow rates, the values of the specific enthalpies and specific entropies of the present study and those of the first reference model [23] are found to be close to one another with minimum relative errors (RE).

A similar comparison of the present study for the second flashing also found minimal errors in the

performance parameters. The comparison results have been shown in table 2.

**Table 1. Validation of the results of present model for first flashing process with Reference model [23].**

State 'i'	T (°C)		p (kPa)		h (kJ/kg)		s (kJ/kg. K)			ṁ (kg/s)			
	Ref. [23]	Present study	Ref [23]	Present study	Ref [23]	Present study	RE (%)	Ref [23]	Present study	RE (%)	Ref [23]	Present study	RE (%)
1	230	230.00	2797.09	2795	990.19	990.00	0.019	2.610	2.6100	0.00	1	1	0.00
2	162.98	163.00	666.5	666.50	990.19	990.00	0.019	2.664	2.664	0.00	1	1	0.00
3	162.98	163.00	666.5	666.50	2760.67	2761.00	0.012	6.723	6.7250	0.029	0.1456	0.1453	0.206
4	98.58	98.61	96.4	96.40	2531.05	2499.00	2.05	6.988	6.9010	0.087	0.1456	0.1453	0.206

**Table 2. Results comparison between present model with Reference model [7] for second flashing process.**

State 'i'	T (°C)		p (kPa)		h (kJ/kg)		s (kJ/kg. K)		ṁ (kg/s)	
	Ref. [7]	Present study	Ref. [7]	Present study	Ref. [7]	Present study	Ref. [7]	Present study	Ref. [7]	Present study
4	370.15	370.15	90.94	90.94	2459	2459	6.818	6.818	87	87
5	424.15	424.15	488.6	488.6	639	640.1	1.858	1.86	513	513
6	370.15	369.87	90.94	90.03	639	640.1	1.901	1.905	513	513
7	370.15	369.87	90.94	90.03	2670	2671	7.388	7.394	53	52.9
8	370.15	370.15	90.94	90.94	2539	2539	7.034	7.034	140	139.9
10	370.15	369.87	90.94	90.03	405	405.2	1.237	1.27	460	460.1

#### 4. Results and discussion

The exergy analysis of the present DFGPP system requires the energy analysis to be performed first to evaluate the energy rate, energy efficiency, and the work output of the turbines and the pump work input. On the other hand, the exergy analysis has given an estimation of the quality of energy utilization by evaluating the exergy destructions in the various components of the system. The present analysis is conducted with similar input parameters as have been considered for the analysis of a single flash geothermal power plant (SFGPP) by Joyshree *et al.* (2023). These parameters for the energy and exergy analysis include mass flow rate, well head temperature, separator temperature, and pump exit pressure, over and above few other assumed parameters which are reported and listed in Section 2.1 in this present study. The results at the states 1 to 4 for the first flashing in the present study has been validated with data of the reference model [23] and are listed in Table 1. Similar comparison for has been made with a reference model [7] to validate the results of the the second flashing process and the comparative data is shown in table 2. The geo-fluid pressure at the reservoir exit is at 2.9 bar, as was obtained in an assessment by Jha and Puppala [24]. Moreover, the mass flow rate of the geo-fluid at the well head was estimated to be at approximately 52.8 kg/s, and the pump exit pressure of 1 bar has been assumed. Further, the steam exiting the reservoir is assumed to be of quality in the range of 0.1-0.15. The computations of the energy and exergy rates at the state points of the DFGPP are subjected to the evaluation of the state thermodynamic properties for the flow streams and are shown in table 3 (see Appendix A). In addition, the state-wise exergy rates of the

flow streams and the specific flow exergy are obtained in Table 4 using the property values and the computed parameters of table 3. The energy and exergy efficiencies are evaluated approximately as 9.52% and 48.39%, respectively.

In table 3, beside the thermodynamic properties of the working fluid, the state-wise energy rates of the flow streams are evaluated by determining the specific enthalpies and entropies at the computed mass flow rates, pressure and, temperatures for the applicable values of steam quality.

In the DFGPP, because of the inlet and outlet fluid conditions and variable mass flow rates, the energy loss rates across different components of the DFGPP system is found to vary. The loss in energy rate is maximum for the condenser with 22957.361 kW, while it is minimum for the mixer M2 followed by mixer M1, LPS/SEP2, pump, HPS/SEP, HPT, and LPT, respectively. The expansion process in the two expansion valves EV1 and EV2 are assumed to be isenthalpic; hence, the energy losses in these valves are zero. The energy loss rates that occurred in the various components of the DFGPP are shown in figure 3 (see Appendix A).

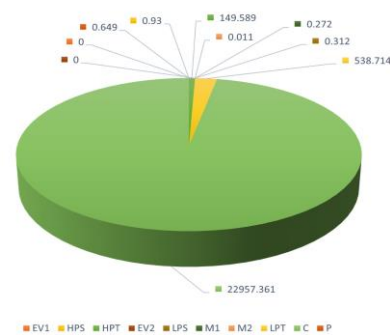


**Figure 3. Energy loss rates across components of the DFGPP in kW.**

From the energy analysis, the work output of the HPT and LPT are evaluated and found to be 847.67 kW and 3052.71 kW respectively while the input work for the pump is about 1.622 kW approximately.

In table 4, the state-wise the specific flow exergy and the exergy rates of the flow streams are shown. In table 4, it has been observed that the exergy flow rates follow a reducing trend from a maximum value of the stream at the well head at state 1 to a lower value at state 7. The exergy rate then increases to state 8, which subsequently decrease to a very low value at state 12, thereafter fluctuating between the states 12 and 15. The mixing of the fluid streams 4 and 7 in the fluid mixer M1 may have resulted in a higher exergy rate output at state 8. Further, from Table 4, a comparison in the exergy rates at the states 5 and 10 showed that the exergy rates of the hot liquid fluid across the HPS is higher than that across the LPS by 820.456 kW and at the states 3 and 7, similar results are observed for the stream of steam, where the exergy rate across the HPS exceeds those of the LPS by a higher value of 4558.879 kW. However, the maximum reduction in exergy flow rates is found to occur across the LPT at 501.5262 kW, whereas an almost negligible reduction has been observed in the LPS, HPS, and the mixing device M1 with approximately 0.0001 kW, 0.0007 kW, and 0.5098 kW, respectively, and are illustrated in figure 4. Moreover, besides the above components, the component-wise exergy destruction rates of the other components of the DFGPP are shown in figure 4. The DFGPP produces a net output work of approximately 3.9 MW.

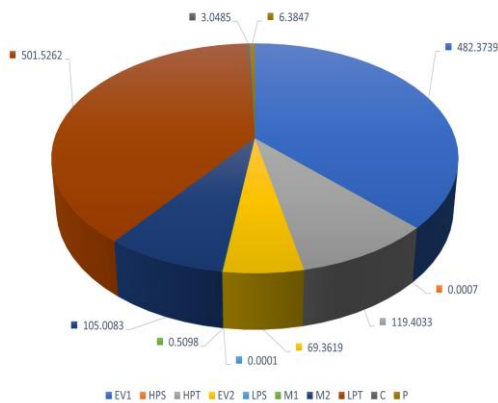


Figure 4. Exergy destruction rates across each component of the DFGPP in kW.

Table 4. Computation of state-wise specific flow exergy and total exergy flow rates of the DFGPP.

State	$\dot{m}$ (kg/s)	$h_0$ (kJ/kg)	$s_0$ (kJ/kg.K)	$e_{xi}$ (kJ/kg, K)	$\dot{e}_i$ (kW)
1	52.700	104.407	0.367	152.891	8057.367
2	52.700	104.407	0.367	143.738	7574.993
3	9.165	104.407	0.367	579.418	5310.079
4	9.165	104.407	0.367	474.112	4345.001
5	43.536	104.407	0.367	52.011	2264.346
6	43.536	104.407	0.367	50.431	2195.551
7	1.543	104.407	0.367	486.844	751.200
8	10.708	104.407	0.367	475.989	5096.649
9	10.708	104.407	0.367	143.752	1539.220
10	41.993	104.407	0.367	34.384	1443.890
11	10.708	104.407	0.367	3.394	36.339
12	10.708	104.407	0.367	2.949	31.577
13	52.700	104.407	0.367	26.014	1370.920
14	542.82	104.407	0.367	0.000	0.000
15	542.82	104.407	0.367	1.277	623.320

In reality, the exergy destruction rate for the two separators are almost zero [8], as can be seen in Fig. 3 and can be proved thermodynamically using the second law of thermodynamics. The rate of entropy generation for each of the two separators is given by equations (13) and (14) as follows:

$$\dot{S}_{gen}|_{HPS} = \dot{m}_3 s_3 + \dot{m}_5 s_5 - \dot{m}_2 s_2 \quad (13)$$

$$\dot{S}_{gen}|_{LPS} = \dot{m}_7 s_7 + \dot{m}_{10} s_{10} - \dot{m}_6 s_6 \quad (14)$$

The substitution of the input parameters into the equations (53) and (54) results in nearly zero entropy generation rate for the two separators i.e.

$$\dot{S}_{gen}|_{sep} = 0 \quad (15)$$

Therefore, the exergy destruction rates are also evidently proved to be approximately zero across both the separators.

## 5. Conclusions

In the present study, the proposed double flash geothermal power plant (DFGPP) model has been and analysed thermodynamically based on the available geo-field conditions in the Puga valley geo-field in the Ladakh region, India. Using the first and second law of thermodynamics, the study evaluates the thermal and the exergetic performance of the plant in terms of energy and exergy performance parameters of the individual components and for the overall plant. Moreover, the geo-thermal plant is operated with 100% condenser effectiveness, and no heat transfer losses, while assuming adiabatic mixing having no pressure loss across the separators and in the mixing devices. The thermodynamic properties of the geo-fluid streams were also determined at the state points of the components of DFGPP for the

system evaluation. The results of the exergetic performance analysis of the DFGPP are summarized in the following:

The rate of energy losses and exergy destructions and the energy and exergetic efficiencies of the components of DFGPP as well as the power output are affected by the location and geological conditions of the geo-fluid at the reservoir and at well head.

There is no loss in energy rates in the two expansion valves due to isenthalpic expansion processes, while it is found to be maximum for the condenser due to maximum enthalpy changes for this component. However, there is least losses in the rate of energy for the two mixing devices with mixer M1 having slightly higher loss compared to mixer M2 followed by the two separators where the loss in HPS/SEP1 separator is higher than that of LPS/SEP2 separator with the pump loss in between the two separators. This may be caused due to higher enthalpy changes between the inlet and exit points in the HPS and M1, as compared to LPS and mixer M2 having different mass flow rates based on the inlet fluid pressures and condition of fluids mixing.

The DFGPP's net work output under the given geo-fluid operating conditions is found to be around 3.9 MW. The computed energy and exergy efficiency for the cycle is found to be 9.52 % 48.39%, respectively.

The actual work output of the LPT is found to be higher with HPT work output being only 27.77% of the LPT work while the isentropic pump work is found to be low at 0.973 kW.

Exergetically, the highest rate of destruction occurred in the LPT, while the minimum in the LPS. However, the overall exergy destruction rate for the DFGPP is about 1.29 MW, as compared to the overall thermal losses of 23.65 MW.

Due to lower overall exergy destruction rate, the DFGPP can be a suitable candidate for geothermal power extraction operating in the Indian geo-field conditions. The operating of the DFGPP for the present geo-fluid conditions is also found suitable due to high exergetic efficiency and low thermal efficiency.

The present study investigated the operation of a geothermal power plant by using the geo-fluid flashing process twice. The use of a DFGPP in the Indian sub-continent for energy extraction from the available geo-fluid possesses the potential to meet the ever growing energy demand. As a future scope, and based upon the Indian geo-fluid conditions, and location, further a combined binary geo-thermal cycle can be investigated to study the power extraction potential from the

available geo-energy. However, such investigations will provide more realistic results when suitable and advanced extraction tools are employed to a maximum extent.

## 6. Acknowledgments

The authors of this study are highly grateful to all the available literary sources and their creators for the significant contributions made in the development of geothermal energy conversion systems. The authors would also like to convey our heartfelt thanks to all the people whose advises has helped in the successful completion of this study.

## 7. Statements and declarations/competing interests

The authors of the manuscript declare that there is no conflict of interest on any matter related to any material, funding or whatsoever concerning the present work from any parties. Moreover, the authors declare that no funds, grants, or other support was received from any organization for the submitted work.

## 8. References

- [1] International Renewable Energy Agency (IRENA) (2018). [https://www.irena.org/media/Files/IRENA/Agency/Publication/2018/Apr/IRENA\\_Report\\_GET\\_2018.pdf](https://www.irena.org/media/Files/IRENA/Agency/Publication/2018/Apr/IRENA_Report_GET_2018.pdf).
- [2] Nardini I (2022). Geothermal Power Generation. In: Hafner M and Luciani G (eds) *The Palgrave Handbook of International Energy Economics*. Palgrave Macmillan, Cham. pp. 183-194. [https://doi.org/10.1007/978-3-030-86884-0\\_11](https://doi.org/10.1007/978-3-030-86884-0_11).
- [3] Zhang LX, Pang MY, Han J, Li YY, and Wang CB (2019). Geothermal power in China: Development and performance evaluation. *Ren Sustain Egy Rev*. 116: 109431. <https://doi.org/10.1016/j.rser.2019.109431>.
- [4] Jeanne P, Rutqvist J, Hartline C, Garcia J, Dobson PF, and Walters M (2014) Reservoir structure and properties from geomechanical modeling and microseismicity analyses associated with an enhanced geothermal system at The Geysers, California. *Geothermics*. 51: 460-469. <https://doi.org/10.1016/j.geothermics.2014.02.003>.
- [5] Luo C, Zhao J, Gong Y, and Ma W (2017). Energy efficiency comparison between geothermal power systems. *Therm Sci*. 21(6): 2633-2642. <https://doi.org/10.2298/TSCI151225074L>.
- [6] Pambudi NA, Itoi R, Jalilinasrabady, and S, Khasani (2013). Performance evaluation of double-flash geothermal power plant at dieng using second law of thermodynamics proceedings, In: *Thirty-Eighth Workshop on Geothermal Reservoir Engineering*

Stanford University, Stanford, California, February 11-13, SGP-TR-198.

[7] Jalilinasrabad S, Valdimarsson P, and Saevarsdottir G (2008) Exergy analysis of double flash geothermal power plant, Sabalan, Iran. In: Proc. of CTSI Clean Technology and Sustainable Industries Conference and Trade Show. pp. 140-143.

[8] Siddiqui O and Dincer I (2019) Exergetic performance investigation of varying flashing from single to quadruple for geothermal power plants. *J. Energy Resour. Technol.* 141(12): 122301. <https://doi.org/10.1115/1.4043748>.

[9] Harinarayana T, Abdul AKK, Murthy DN, Veeraswamy K, Rao SPE, Manoj C, and Naganjaneyulu K (2006). Exploration of geothermal structure in Puga geothermal field, Ladakh Himalayas, India by magnetotelluric studies. *J. Appl. Geophys.* 58: 280-295. <https://doi.org/10.1016/j.jappgeo.2005.05.005>.

[10] Puppala H and Jha SK (2019) Extraction schemes to harness geothermal energy from puga geothermal field, India. *Energy sources, Part A: Recov. Utilization and Env. Effects.* 43 (5): 1912-1932. <https://doi.org/10.1080/15567036.2019.1668086>.

[11] Jha SK and Puppala H (2018) Conceptual modeling and characterization of Puga geothermal reservoir, Ladakh, India. *Geothermics.* 72: 326-337. <https://doi.org/10.1016/j.geothermics.2017.12.004>.

[12] Jha SK, Puppala H, and Kumar MSM (2020). 3D characterization of thermo-hydro-geological fields and estimation of power potential from Puga geothermal reservoir, Ladakh, India. *Renew. Egy.* 146: 1510-1523. <https://doi.org/10.1016/j.renene.2019.07.006>.

[13] Absar A, Kumar V, Bajpai I, Sinha AK, and Kapoor A (1996) Reservoir modelling of Puga geothermal system, Ladakh, Jammu and Kashmir. *Geology.* 45: 69-74.

[14] Abdul AKK and Harinarayana T (2007). Magnetotelluric evidence of potential geothermal resource in Puga, Ladakh, NW Himalaya. *Curr. Sci.* 93(3): 323-329. [https://www.researchgate.net/publication/228372106\\_Magnetotelluric\\_evidence\\_of\\_potential\\_geothermal\\_resource\\_in\\_Puga\\_Ladakh\\_NW\\_Himalaya](https://www.researchgate.net/publication/228372106_Magnetotelluric_evidence_of_potential_geothermal_resource_in_Puga_Ladakh_NW_Himalaya).

[15] Harinarayana T, Abdul AKK, Murthy DN, Veeraswamy K, Rao SPE, Manoj C, and

Naganjaneyulu K (2006). Exploration of geothermal structure in Puga geothermal field, Ladakh Himalayas, India by magnetotelluric studies. *J. Appl Geophys.* 58: 280-295.

<https://doi.org/10.1016/j.jappgeo.2005.05.005>.

[16] Kumar R, Singh M, Gupta L, and Rao GV (1982). Geophysical surveys in Parvati valley geothermal field, Kullu, India. 13(3): 213-222. [https://doi.org/10.1016/0377-0273\(82\)90051-8](https://doi.org/10.1016/0377-0273(82)90051-8).

[17] Akpan A, Narayanan M, and Tirumalachetty, H (2014). Estimation of subsurface temperatures in the Tattapani Geothermal Field, Central India, from limited volume of magnetotelluric data and borehole thermograms using a constructive back-propagation neural network. *Earth Interact.* 18 (6): 1-26. DOI:10.1175/2013EI000539.1.

[18] Singh H, Chandrasekharam D, Gurav T, and Singh B (2015). Geochemical characteristics of Bakreswar and Tantloi geothermal province, India. *World Geothermal Congress, Melbourne, Australia, April 19-25*, pp. 1-5.

[19] Chauhan V, Anil Kishan P, and Gedupudi S (2019). Thermodynamic analysis of a combined cycle for cold storage and power generation using geothermal heat source. *Therm. Sc. Engg. Prog.* 11: 19-27.

[20] Chouhan M and Barange SK (2020). Assessment of technical feasibility based on thermo-exergic analysis for proposed binary cycle power plant for Tatapani geothermal field. *Int. J. Resr Engg Appln. & Mgmt.* 6 (3): 337-348.

[21] Bejan A, Tsatsaronis G, and Moran M (1996). *Thermal Design and Optimization.* John Wiley & Sons Inc, USA.

[22] Kotas TJ (2012). *The Exergy Method of Thermal Plant Analysis.* Exergon Publishing Company Ltd, UK.

[23] Wang J, Wang J, Dai Y, and Zhao P (2015). Thermodynamic analysis and optimization of a flash-binary geothermal power generation system. *Geothermics.* 55: 69-77. <https://doi.org/10.1016/j.geothermics.2015.01.012>.

[24] Jha SK and Puppala H (2017) Assessment of subsurface temperature distribution from the gauged wells of Puga Valley, Ladakh. *Geotherm. Egy.* 5(3): 1-15. <https://doi.org/10.1186/s40517-017-006-4>.

## Appendix A. Mathematical equations for energy and exergy analysis

### a) Energy analysis

#### Conservation equations:

##### (i) Equations of mass balance:

$$\dot{m}_1 = \dot{m}_2 = \dot{m}_{13} \quad (16)$$

$$\dot{m}_3 = \dot{m}_4 = x_2 \dot{m}_2 \quad (17)$$

$$\dot{m}_5 = \dot{m}_6 = (1 - x_2) \dot{m}_2 \quad (18)$$

$$\dot{m}_7 = x_6 \dot{m}_6 \quad (19)$$

$$\dot{m}_{10} = (1 - x_6) \dot{m}_6 \quad (20)$$

$$\dot{m}_8 = \dot{m}_4 + \dot{m}_7 \quad (21)$$

$$\dot{m}_8 = \dot{m}_9 = \dot{m}_{11} = \dot{m}_{12} \quad (22)$$

$$\dot{m}_{13} = \dot{m}_{12} + \dot{m}_{10} \quad (23)$$

##### (ii) Equations of energy balance:

Expansion Valve 1 (EV1):

$$h_1 = h_f|_{T_1} + x_1 h_{fg}|_{T_1} \quad (24)$$

$$x_2 = \frac{h_2 - h_f|_{T_2}}{h_{fg}|_{T_2}} \quad (25)$$

High pressure separator (HPS/SEP1):

$$h_3 = h_g|_{T_{HPS}} \quad (26)$$

$$h_5 = h_f|_{T_{HPS}} \quad (27)$$

High pressure turbine (HPT):

$$x_{4s} = \frac{s_{4s} - s_f|_{T_4}}{s_{fg}|_{T_4}} \quad (28)$$

$$s_{4s} = s_3 = s_g|_{T_{sep}} \quad (29)$$

$$h_{4s} = h_f + x_{4s} h_{fg} \quad (30)$$

Expansion valve 2 (EV2):

$$h_5 = h_6 \quad (31)$$

$$x_6 = \frac{h_6 - h_f|_{T_6}}{h_{fg}|_{T_6}} \quad (32)$$

Low pressure separator (LPS/SEP2):

$$h_7 = h_g|_{T_7} \quad (33)$$

$$h_{10} = h_f|_{T_7} \quad (34)$$

Mixing chamber (M1):

$$h_8 = \frac{\dot{m}_7 h_7 + \dot{m}_4 h_4}{\dot{m}_7 + \dot{m}_4} \quad (35)$$

$$x_8 = \frac{h_8 - h_f|_{T_8}}{h_{fg}|_{T_8}} \quad (36)$$

$$s_8 = s_f|_{T_8} + x_8 s_{fg}|_{T_8} \quad (37)$$

$$s_{9s} = s_8 \quad (38)$$

Low pressure turbine (LPT):

$$\dot{W}_{LPT} = \dot{m}_8 (h_8 - h_9) \quad (39)$$

$$h_9 = h_8 - \eta_T (h_8 - h_{9s}) \quad (40)$$

$$h_{9s} = h_f|_{T_9} + x_{9s} h_{fg}|_9 \quad (41)$$

Condenser:

$$\dot{Q}_C = \dot{m}_9(h_{11} - h_9) \quad (42)$$

$$h_{11} = h_f|_{P_{\text{cond}}} \quad (43)$$

Pump:

$$s_{12s} = s_{11} \quad (44)$$

$$h_{12s} - h_{11} = v_{11}(P_{12} - P_{11}) \quad (45)$$

**(b) Exergy balance equations:**

Expansion valve 1(EV1):

$$\dot{\epsilon}_1 = \dot{\epsilon}_2 + \dot{\epsilon}_{d,v_1} \quad (46)$$

High pressure separator (HPS/SEP1):

$$\dot{\epsilon}_2 = \dot{\epsilon}_3 + \dot{\epsilon}_5 + \dot{\epsilon}_{d,HPS} \quad (47)$$

High pressure turbine (HPT):

$$\dot{\epsilon}_3 = \dot{\epsilon}_4 + \dot{W}_{HPT} + \dot{\epsilon}_{d,HPT} \quad (48)$$

Expansion valve 2 (EV2):

$$\dot{\epsilon}_5 = \dot{\epsilon}_6 + \dot{\epsilon}_{d,v_2} \quad (49)$$

Low pressure separator (LPS/SEP2):

$$\dot{\epsilon}_6 = \dot{\epsilon}_7 + \dot{\epsilon}_{10} + \dot{\epsilon}_{d,LPS} \quad (50)$$

Mixing chamber (M1):

$$\dot{\epsilon}_7 + \dot{\epsilon}_4 = \dot{\epsilon}_8 + \dot{\epsilon}_{d, M1} \quad (51)$$

Low pressure turbine (LPT):

$$\dot{\epsilon}_8 = \dot{\epsilon}_9 + \dot{W}_{LPT} + \dot{\epsilon}_{d,LPT} \quad (52)$$

Condenser:

$$\dot{\epsilon}_9 = \dot{\epsilon}_{11} + \dot{\epsilon}_{d,cond} \quad (53)$$

Pump:

$$\dot{\epsilon}_{11} + \dot{W}_P = \dot{\epsilon}_{12} + \dot{\epsilon}_{d,P} \quad (54)$$

Mixing chamber (M2):

$$\dot{\epsilon}_{10} + \dot{\epsilon}_{12} = \dot{\epsilon}_{13} + \dot{\epsilon}_{d, M2} \quad (55)$$

**Table 3. Thermodynamic properties and energy rates of working geofluid (water) at state ‘i’.**

State	T (°C)	P (bar)	h (kJ/kg)	s (kJ/kg. K)	ṁ (kg/s)	Ẽ <sub>i</sub> (kW)	x
1	132.370	2.900	881.675	2.462	52.700	46464.270	0.150
2	118.596	1.900	881.675	2.492	52.700	46464.270	0.174
3	118.596	1.900	2704.200	7.144	9.165	24782.640	1.000
4	99.606	1.000	2611.923	7.187	9.165	23936.970	0.972
5	118.596	1.900	498.000	1.513	43.536	21680.700	0.000
6	99.606	1.000	498.000	1.518	43.536	21680.700	0.035
7	99.606	1.000	2675.400	7.357	1.543	4128.142	1.000
8	99.606	1.000	2621.045	7.212	10.708	28064.840	0.976
9	45.840	0.100	2335.945	7.369	10.708	25012.130	0.896
10	99.606	1.000	418.000	1.304	41.993	17552.870	0.000
11	45.840	0.100	191.900	0.649	10.708	2054.769	0.000
12	45.969	1.000	192.052	0.651	10.708	2056.391	-
13	88.708	1.000	372.092	1.178	52.700	19609.250	-
14	25.000	1.013	104.407	0.367	542.820	56673.900	-
15	35.000	1.013	146.700	0.505	542.820	79631.300	-